Observation of interatomic Coulombic decay and electron-transfer-mediated decay in high-energy electron-impact ionization of Ar_2

S. Yan,[1] P. Zhang,[1] X. Ma,[1,*] S. Xu,[1] B. Li,[1] X. L. Zhu,[1] W. T. Feng,[1] S. F. Zhang,[1] D. M. Zhao,[1] R. T. Zhang,[1] D. L. Guo,[1,2] and H. P. Liu[1]

[1]*Institute of Modern Physics, Chinese Academy of Sciences, Lanzhou 730000, China*

[2]*University of Chinese Academy of Sciences, Beijing 100049, China*

(Received 25 June 2013; published 29 October 2013)

We measured the kinetic energy distributions of the fragment ions of doubly and quadruply ionized argon dimers using 3000 eV electron impact. For the dissociation of $(Ar_2)^{2+}$, the peak that indicates radiative charge transfer is observed, where the outer-shell ionization (dominant in highly charged ion collision) and the inner-shell ionization (preferential in x-ray experiments) have approximately equal contributions. For the dissociation of $(Ar_2)^{4+}$, the interatomic Coulombic decay and electron-transfer-mediated decay are first observed in the electron-impact process.

DOI: 10.1103/PhysRevA.88.042712 PACS number(s): 34.80.Gs, 34.70.+e, 36.40.−c, 82.33.Fg

I. INTRODUCTION

Van der Waals clusters have attracted considerable interest because they are bonded by weak polarization forces and characterized by larger internuclear distances than ordinary molecules. Therefore, they are the best candidates to study the new phenomena that emerge in the environment formed by separated neighboring atoms [1–15]. Since the pioneering work of Cederbaum *et al*. [1] in 1997, numerous experiments that aim to identify a new mechanism, which is termed the interatomic Coulombic decay (ICD), have been performed, and several other decay mechanisms of highly charged, loosely bound systems have also been predicted and investigated using synchrotron radiation, such as the electron-transfer-mediated decay (ETMD), and the radiative-charge-transfer (RCT) decay. Simultaneously, the distributions of the kinetic energy release (KER, which is the sum of the kinetic energies of all fragment ions) and the branching ratios of different decay channels become good observables to distinguish the mechanisms from one another.

Different decay mechanisms are schematically shown in Fig. 1 for a loosely bound system of atoms A and B. If an initial vacancy is created in an inner shell of atom A and if the drop of an outer-shell electron into the vacancy does not yield sufficient excess energy to ionize another bound electron in atom A the ICD process will tend to be invoked; i.e., the excess energy will be transferred to the neighboring atom B via virtual photons, and one outer-shell electron of atom B will be ionized [1] [see Fig. 1(a)]. The indication of ICD was first observed by Marburger *et al*. [2] in a photoionization experiment with Ne clusters, and the unambiguous evidence of ICD was provided by Jahnke *et al*. [3] in a 2*s* ionized neon dimer. Following these experiments, many studies suggested that ICD processes should generally exist in homonuclear and heteronuclear rare gas clusters [4,5] and in hydrogen-bonded molecular clusters [6]. Figure 1(b) shows another electronic deexcitation channel, the ETMD, where the vacancy in the initially ionized or excited atom A is filled by the valence electron from the neighboring atom B, and the excess energy is released by ionizing another valence electron of atom B [7]. The conclusive experimental evidence of the ETMD process was first obtained by Sakai *et al*. [8] from the triply charged states in the Ar dimer using the triple coincidence technique in $2p$ inner-shell photoionization. Simultaneously, a new ETMD pathway in mixed Ar-Kr clusters was investigated by Förstel *et al*. [9], where the charge transfer of a third neighboring atom is involved. It is clear that the decay processes are so fast that the effect of nuclear motion can be ignored in both ICD and ETMD [10,11]. As shown in Fig. 1(c), for a system that consists of a highly charged ion A in the ground state or a low-lying excited state, if the entire system is populated in a high vibrationally excited state, the RCT process may occur; i.e., one bound electron of the neighboring atom B will be transferred to ion A, then the residual energy is released via photon emission [12]. According to the Auger electron spectra, Saito *et al*. [13] first demonstrated that the RCT process was the dominant decay mechanism of the one-site doubly ionized states Ar^{2+}-Ar, which are induced by an Auger decay from the inner-shell photoionization of $Ar^{+}(2p^{-1})$-Ar.

All of the experiments mentioned above focused on the fragmentation mechanism that is induced from one-site inner-shell electron ionization using synchrotron radiation. In contrast, recently, some other investigations have been performed to study the role of the multiple ionization of outer-shell electrons using intense femtosecond lasers [14,15] or low-energy highly charged ions (HCI) [16]. For the intense femtosecond laser impact, a fragmentation mechanism that follows a two-site sequential ionization was suggested. In this mechanism, one valence electron is emitted via tunnel ionization of any constituent atom, and the neighboring atom can be ionized by the rescattering of the emitted electron in the laser field or by the sequential tunnel ionization that the neighboring ion mediates [14]. In contrast, for the highly charged ion impact, the intensity of the projectile Coulomb field is sufficiently large to evoke multiple captures (ionizations) of each constituent during an ultrashort time period. This results in the sequential two-site multiple-capture (ionization); i.e., several outer-shell electrons are removed from each atom sequentially as the projectile skims across the cluster.

Considering all of the investigations mentioned above, a question can naturally be raised: Could a new type of experiment be performed to activate all of the above mechanisms and display the competition among ICD, ETMD, RCT, and

*Corresponding author: X.ma@impcas.ac.cn

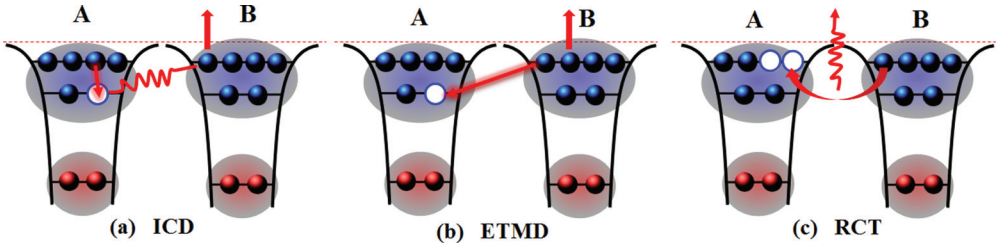

FIG. 1. (Color online) Schematic diagram of different decay channels. (a) ICD process, (b) ETMD process, (c) RCT process. See text for the details.

two-site multiple ionization? Because the high-energy electron can evoke the fragmentation channels from both the single inner-shell vacancy and the sequential ionization of outer-shell electrons, most of the decay channels that are explored in the HCI and x-ray experiments can be investigated simultaneously. From the KER distribution of the fragments and the relative cross sections of the different mechanisms, the competition among different decay pathways can be explored. Therefore, the investigation of the fragmentation induced by high-energy electron impact is considered an excellent candidate to answer the above question.

Although several experiments that focused on the dissociative ionization dynamics of small clusters by low-energy electron impact were performed [17–21], the corresponding incident energies were not sufficiently large to produce an inner-shell vacancy. In the present article, we report an experiment that emphasizes the fragmentation mechanisms of multiply charged Ar dimer ion induced by high-energy electron. The momentum distributions of the fragments were measured in coincidence, and the KER distributions of Ar^+-Ar^+, Ar^+-Ar^{3+}, and Ar^{2+}-Ar^{2+} ion pairs were obtained. The evidence of ICD, ETMD, and RCT processes were observed.

II. EXPERIMENT

The experiment was performed using reaction microscope at the Institute of Modern Physics CAS, Lanzhou [22,23]. Briefly, it is composed of a pulsed electron gun, a two-stage supersonic gas jet system, a recoil ion detector with delay-line anode, a Faraday cup, a time-of-flight spectrometer (ToF), and a Helmholtz coil used to construct a magnetic lens. The pulsed electron beam with a kinetic energy of 3000 eV and a pulse width of 40 ns at 50 kHz repetition rate is provided by the electron gun. After being confined by the magnetic lens, the pulsed electron beam collides with the argon cluster target, which is produced by expanding Ar gas with a 2-bar stagnation pressure through a nozzle ($\phi = 30\ \mu$m), and the fraction of dimers is approximately 1% of the monomer Ar. After single or multiple ionization of inner- or outer-shell electrons from an Ar dimer, the initial ion states are produced, then Coulombic explosion of the parent ions will be evoked through the energy- and charge-transfer processes. The recoil ions induced from the Coulombic explosion are extracted and accelerated towards the recoil ion detector using the electrostatic field E (83.5 V/cm). The corresponding flight time and position information will be sorted using the PXI (PCI extensions for instrumentation)-based acquisition system. The momentum of each ion is reconstructed in an offline analysis. The residual beam is collected into a Faraday cup. Because the correlated charged fragments from highly charged dimers always fly back to back, the momentum conservation law can be imposed to suppress the background ions produced from monomer ionization and larger cluster ionization. The resolution of the KER spectrum from the fragmentation of $(Ar_2)^{2+}$ is less than 0.1 eV.

III. RESULTS AND DISCUSSION

Due to the high speed of the impact electrons, the ionization process should be governed by the Franck-Condon principle: The electrons make a vertical transition to the ionization state in the first step, while the nuclei retain their positions and momenta. After ionization, the nuclei that displace to the equilibrium distance will experience polarization forces, and the geometry evolution begins in the second step. Finally, the cluster ion will split into several charged separations. Because of Coulomb repulsion, charged fragments depart from each other in high kinetic energy (Coulombic explosion). Under the present impact energy, ionization of all shells of the Ar atom can be opened in the first step. However, because the ionization cross section of the K shell (10^{-22} cm^2) is at least three orders lower than that of the L shell ($>9 \times 10^{-19}$ cm^2) for Ar atom [24], it is reasonable to ignore the contribution of the $1s$ electron ionization in the following discussion.

The KER distribution of the Ar^+-Ar^+ ion pairs, which were produced from the doubly charged Ar dimer ion, is shown in Fig. 2 and obviously, two peaks appear. One peak is located at 3.7 eV (peak A), and the other peak is at approximately 5.3 eV

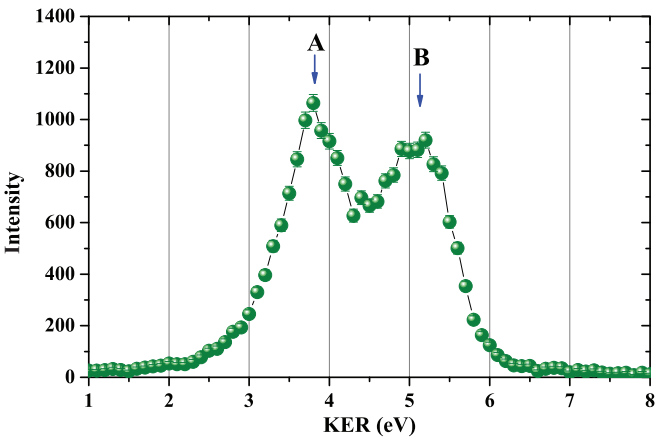

FIG. 2. (Color online) KER distribution of the Ar^+-Ar^+ pair from $(Ar_2)^{2+}$ ions. The vertical axis represents the ion yields (the corresponding unit is counts).

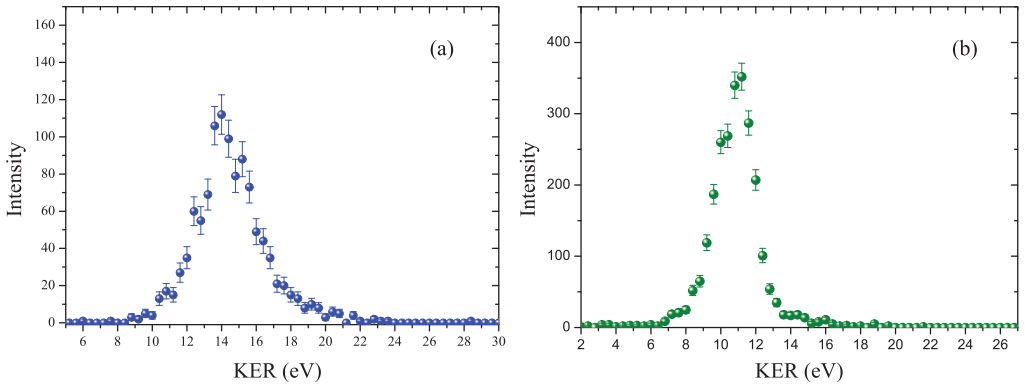

FIG. 3. (Color online) (a) KER distribution of the Ar^{2+}-Ar^{2+} pair from $(Ar_2)^{4+}$ ions, (b) KER distribution of the Ar^{+}-Ar^{3+} pair from $(Ar_2)^{4+}$ ions. The vertical axis represents the ion yields (the corresponding unit is counts).

(peak B). These peak positions are consistent with the results obtained by low-energy electron, laser, and highly charged ion impacts; see Refs. [15,16,21]. The ratios of intensity of peak B to that of peak A in each of the experiments are different, in the laser experiment, the magnitude of peak B is at least one order lower than that of peak A. For highly charged ion and low-energy-electron experiments, the ratio is about 0.7. However, the value extracted from the present experiment is larger than 0.8, the largest comparing with all the above values. In a classical reflection approximation [25], the KER of the Coulombic explosion (CE) is given by KER $\propto (Z_1 Z_2)/R$, where Z_1, Z_2, and R denote the charges of the first detected ion, the charges of the second detected ion, and the distance between the two point charges at the instant of explosion, respectively. If Z_1 and Z_2 are known, the internuclear distance can be deduced from KER.

Peak A corresponds to the CE that occurs at an internuclear distance of 3.8 Å, which is the equilibrium internuclear distance of the Ar dimer. This indicates that the CE process happens so quickly that the geometry evolution of the nuclei can be ignored, which indicates that ICD or the two-site double ionization of Ar dimer occurs. In contrast, peak B corresponds a distance of 2.8 Å, which is much shorter than the equilibrium distance. This peak indicates that the lifetime of the initial state is so long that the movements of two nuclei may be fully involved in the fragmentation dynamics. This characteristic is consistent with the occurrence of the RCT process.

As shown in Fig. 1(c), for the RCT process, the initial long-lifetime one-site double-ionized state Ar^{2+}-Ar must be produced before CE happens. The initial state Ar^{2+}-Ar can be formed via the following two processes. One process is the direct double ionization of the outer-shell electrons of one constituent atom in the Ar dimer; the other one is the inner-shell ($2p$ or $2s$) single ionization, which quickly falls into the Ar^{2+}-Ar states via Auger decay. Saito *et al.* [13] systematically investigated the latter one using an x ray with an energy of 245 eV. They found that the KER profiles did not depend on the Auger electron energies, and all peaks of the KER distributions were located at 5.3 eV; they concluded that most of the intermediate states decay via RCT. Pflüger *et al.* [21] investigated the fragmentation process of the doubly ionized state Ar^{2+}-Ar that was produced from direct double ionization using low-energy electron impact, and the evidences of the breakup of $(Ar_2)^{2+}$ dictation via RCT were revealed.

We are interested in the relative contributions of different initial states to RCT. For the isolated Ar atom, the production ratio of the double ionization states $Ar^{2+}(3p^{-2})$ and $Ar^{2+}(3s^{-1}3p^{-1})$ and the intermediate single state $Ar^{+}(2p^{-1})$ using 3000-eV electron impact is 6:1:9 [26]. Thus, for peak B, the relative contribution of the direct double ionization process should be 7/9 that of the inner-shell ionization following the Auger decay. Therefore, if the Ar dimer is doubly charged, the outer-shell ionization and the inner-shell ionization induce approximately equal contributions to RCT. However, when the Ar dimer is quadruply ionized, the contribution of inner-shell ionization is dominant, as shown in the following discussion.

The KER distribution of the symmetrical channel Ar^{2+}-Ar^{2+} and the asymmetrical channel Ar^{3+}-Ar^{+} ion pairs from initially quadruply ionized Ar dimers are shown in Figs. 3(a) and 3(b), respectively. For the symmetrical channel, a peak located at 14.5 eV is observed; it corresponds to an internuclear distance of approximately 3.8 Å and is consistent with the equilibrium internuclear distance of the neutral Ar dimer (3.76 Å). This reveals that there is no sufficient time to couple the nucleus motion into the fragmentation dynamics. The peak resulting from RCT process which should appear at larger KER position is not shown up.

The possible origins of the peak located at 14.5 eV can be attributed to two processes: the sequential two-site quadruple ionization of the Ar dimer and the ETMD process of the one-site triply ionized state Ar^{3+}-Ar. The sequential ionization mechanism can be intuitively described as follows: Two neutral constituents are sequentially doubly ionized; i.e., the outer-shell electrons in atom A become doubly ionized in the first (e, $3e$) process, then the scattered electron or the ionized electron collides with the neighboring atom B and ionizes two of its bound electrons in the second (e, $3e$) process.

The total cross section of this sequential ionization is determined by the cross section of the first (e, $3e$) process and the probability of the second (e, $3e$) process. To ensure that the second (e, $3e$) process occurs, after the first (e, $3e$) process, the scattered or ionized electrons should go through the area that is covered by a spherical shell, whose radius equals to the internuclear distance of the Ar dimer, and the

area is estimated to be 1.7×10^{-14} cm^2 (S_1). If the cross section of the second (e, $3e$) process is S_2, then the probability of the second (e, $3e$) process is determined by the ratio of S_2 to S_1. Because the energies of the scattered electron and the ionized electron are uncertain, here we only estimate the upper limit of the probability. We assume that in the first (e, $3e$) process, each of the two ionized electrons has 100 eV energy, where the cross section of Ar (e, $3e$) is maximum (2.9×10^{-17} cm^2) [26]. Then, in the second (e, $3e$) process, the corresponding cross section of the two impact electrons should be 5.8×10^{-17} cm^2 (S_2). Meanwhile, because the cross section of the second (e, $3e$) process that is induced by the scattered electron impact is one order lower than 2.9×10^{-17} cm^2, the contribution of the scattered electron impact can be safely ignored. The corresponding maximum probability of the second (e, $3e$) process induced by the ionized electrons is estimated to be 0.34%. Considering that the yield ratio of Ar^{2+} to Ar^{4+} is approximately 20:1, the cross section of the one-site quadruply ionized state Ar^{4+}-Ar will be 15 times larger than that of the two-site quadruply ionized state Ar^{2+}-Ar^{2+}. These estimations show that the contribution of the sequential ionization is at least one order lower than that of the one-site quadruple ionization, which results in the RCT process. As clearly seen from Fig. 3(a), the contribution of RCT process is not observable in our KER spectrum. Thus, we may conclude that the relative contribution of the initial two-site quadruply ionized state Ar^{2+}-Ar^{2+} can be safely ignored.

Consequently, we consider that the peak in Fig. 3(a) is the result of the ETMD process of the one-site triply ionized state Ar^{3+}-Ar. In other words, the one-site triply charged state with an inner-valence $3s$ vacancy $Ar^{3+}(3s3p^4)$-Ar is created in the first step; then, the $3s$ vacancy is filled by the $3p$ valence electron of the neighboring atom and results in $Ar^{3+}(3s3p^4)$-Ar $\xrightarrow{\text{ETMD}}$ $Ar^{2+}(3p^4)$-$Ar^{2+}(3p^4)$.

Now we discuss the asymmetrical channel Ar^{3+}-Ar^{+} ion pairs, the KER of which is shown in Fig. 3(b). One obvious peak at 11.5 eV is observed, and the corresponding internuclear distance is approximately 3.8 Å, which is consistent with the equilibrium internuclear distance of the neutral Ar dimer (3.76 Å).

There are two processes that may result in this peak: The CE process, which results from the sequential two-site quadruple ionization of the Ar dimer, and the ICD process of the one-site triply ionized state $Ar^{3+}(3s3p^4)$-Ar. For the sequential ionization, two neutral constituents are ionized sequentially; i.e., the single (triple) ionization of the outer-shell electrons in one constituent atom occurs in the first step, then the scattered electron or the ionized electron collides with the neighboring atom and leads to the triple (single) ionization in the second step. By introducing the same procedure for the cross-section estimation of the sequential ionization, we exclude the contribution of the two-site quadruply ionized state Ar^{3+}-Ar^{+} because its cross section is extremely small compared to that of the one-site quadruply ionized state Ar^{4+}-Ar.

Therefore, the only origin of the peak is attributed to the ICD process of the initial one-site triply ionized state Ar^{3+}-Ar, where an inner-valence $3s$ vacancy $Ar^{3+}(3s3p^4)$-Ar is created in the first step, and in the following step, the $3s$ vacancy of the $Ar^{3+}(3s3p^4)$ ion is filled by one of its own outer-shell electrons, and one outer-shell electron of atom B is ionized. Consequently, the charge state of constituent A remains the same, and the charge state of constituent B increases by one charge unit. Then, $Ar^{3+}(3s3p^4)$-Ar $\xrightarrow{\text{ICD}}$ $Ar^{3+}(3p^3)$-$Ar^{+}(3p^5)$.

Recently, the two interatomic energy relaxation processes were also observed using x-ray impact. Sakai *et al.* [8] investigated ICD and ETMD from the one-site triply charged state $Ar^{3+}(3s3p^4)$-Ar with a $3s$ vacancy, which is produced from Auger decays or direct triple ionization using 345.5-eV energy photon impact. It should be emphasized that many similarities between the two works are observed, such as the shapes of the KERs and the positions of the peaks, and the intensity ratio of the asymmetric channel (Ar^{3+}-Ar^{+}) to the symmetric channel (Ar^{2+}-Ar^{2+}) is approximately 2, in both our result and the ones from the x-ray experiment. These similarities further confirm that the asymmetric channel Ar^{3+}-Ar^{+} and the symmetric channel Ar^{2+}-Ar^{2+} in the present results are mainly produced from ICD and ETMD, respectively.

IV. SUMMARY

In conclusion, using the reaction microscope technique, we have performed the first fragmentation experiment in 3000-eV electron impact on small Ar clusters. The KER distributions of the dissociation of doubly and quadruply ionized argon dimers are obtained. This is the first paper focusing on the roles of different shells in each fragmentation mechanism. For the dissociation of $(Ar_2)^{2+}$, the peak corresponding to the RCT process is observed, where the outer-shell ionization (dominant in highly charged ion collision) and the inner-shell ionization (preferential in x-ray experiments) have approximately equal contributions. However, for the dissociation of $(Ar_2)^{4+}$, the contribution of inner-shell ionization is dominant, and the fragmentation mechanisms of ICD and ETMD are observed for the first time in an electron collision experiment.

ACKNOWLEDGMENTS

This work is supported by the 973 Program of China through Grant No. 2010CB832902, West Light Doctoral Foundation of CAS, the NSFC through Grant No. 10979007, and the Knowledge Innovation Program of CAS through Grant No. KJCX1-YW-N30.

[1] L. S. Cederbaum, J. Zobeley, and F. Tarantelli, Phys. Rev. Lett. **79**, 4778 (1997).

[2] S. Marburger, O. Kugeler, U. Hergenhahn, and T. Moller, Phys. Rev. Lett. **90**, 203401 (2003).

[3] T. Jahnke, A. Czasch, M. S. Schöffler, S. Schössler, A. Knapp, M. Käsz, J. Titze, C. Wimmer, K. Kreidi, R. E. Grisenti, A. Staudte, O. Jagutzki, U. Hergenhahn, H. Schmidt-Böcking, and R. Dörner, Phys. Rev. Lett. **93**, 163401 (2004).

[4] Y. Morishita, X.-J. Liu, N. Saito, T. Lischke, M. Kato, G. Prümper, M. Oura, H. Yamaoka, Y. Tamenori, I. H. Suzuki, and K. Ueda, Phys. Rev. Lett. **96**, 243402 (2006); T. Aoto, K. Ito, Y. Hikosaka, E. Shigemasa, F. Penent, and P. Lablanquie, *ibid.* **97**, 243401 (2006).

[5] T. Ouchi, K. Sakai, H. Fukuzawa, I. Higuchi, Ph. V. Demekhin, Y.-C. Chiang, S. D. Stoychev, A. I. Kuleff, T. Mazza, M. Schöffler, K. Nagaya, M. Yao, Y. Tamenori, N. Saito, and K. Ueda, Phys. Rev. A **83**, 053415 (2011).

[6] T. Jahnke, H. Sann, T. Havermeier, K. Kreidi, C. Stuck, M. Meckel, M. Schöffer, N. Neumann, R. Wallauer, S. Voss, A. Czasch, O. Jagutzki, A. Malakzadeh, F. Afaneh, Th. Weber, H. Schmidt-Böcking, and R. Dörner, Nat. Phys. **6**, 139 (2010).

[7] J. Zobeley, R. Santra, and L. S. Cederbaum, J. Chem. Phys. **115**, 5076 (2001).

[8] K. Sakai, S. Stoychev, T. Ouchi, I. Higuchi, M. Schöffler, T. Mazza, H. Fukuzawa, K. Nagaya, M. Yao, Y. Tamenori, A. I. Kuleff, N. Saito, and K. Ueda, Phys. Rev. Lett. **106**, 033401 (2011).

[9] M. Förstel, M. Mucke, T. Arion, A. M. Bradshaw, and U. Hergenhahn, Phys. Rev. Lett. **106**, 033402 (2011).

[10] C. Buth, R. Santra, and L. S. Cederbaum, J. Chem. Phys. **119**, 10575 (2003).

[11] I. B. Müller and L. S. Cederbaum, J. Chem. Phys. **122**, 094305 (2005).

[12] R. Johnsen and M. A. Biondi, Phys. Rev. A **18**, 996 (1978).

[13] N. Saito, Y. Morishita, I. H. Suzuki, S. D. Stoychev, A. I. Kuleff, L. S. Cederbaum, X. J. Liu, H. Fukuzawa, G. Prümper, and K. Ueda, Chem. Phys. Lett. **441**, 16 (2007).

[14] B. Ulrich, A. Vredenborg, A. Malakzadeh, M. Meckel, K. Cole, M. Smolarski, Z. Chang, T. Jahnke, and R. Dörner, Phys. Rev. A **82**, 013412 (2010).

[15] B. Manschwetus, H. Rottke, G. Steinmeyer, L. Foucar, A. Czasch, H. Schmidt-Böcking, and W. Sandner, Phys. Rev. A **82**, 013413 (2010).

[16] J. Matsumoto, A. Leredde, X. Flechard, K. Hayakawa, H. Shiromaru, J. Rangama, C. L. Zhou, S. Guillous, D. Hennecart, T. Muranaka, A. Mery, B. Gervais, and A. Cassimi, Phys. Rev. Lett. **105**, 263202 (2010).

[17] U. Buck and H. Meyer, Phys. Rev. Lett. **52**, 109 (1984).

[18] D. Bonhommeau, N. Halberstadt, and A. Viel, J. Chem. Phys. **124**, 184314 (2006).

[19] D. Bonhommeau, N. Halberstadt, and U. Buck, Int. Rev. Phys. Chem. **26**, 353 (2007).

[20] T. Pflüger, A. Senftleben, X. Ren, A. Dorn, and J. Ullrich, Phys. Rev. Lett. **107**, 223201 (2011).

[21] T. Pflüger, http://archiv.ub.uni-heidelberg.de/volltextserver/13325/

[22] S. Yan, X. Ma, P. Zhang, S. Xu, S. F. Zhang, X. L. Zhu, W. T. Feng, and H. P. Liu, Phys. Rev. A **82**, 052702 (2010).

[23] J. Ullrich, R. Moshammer, A. Dorn, R. Dörner, L. Ph. H. Schmidt, and H. Schmidt-Böcking, Rep. Prog. Phys. **66**, 1463 (2003).

[24] S. Segui, M. Dingfelder, and F. Salvat, Phys. Rev. A **67**, 062710 (2003).

[25] E. A. Gislason, J. Chem. Phys. **58**, 3702 (1973).

[26] L. K. Jha, S. Kumar, and B. N. Roy, Eur. Phys. J. D **40**, 101 (2006).